Optimized algorithm for the spatial nonuniformity correction of an imaging system based on a charge-coupled device color camera

Marta de Lasarte, Jaume Pujol, Montserrat Arjona, and Meritxell Vilaseca

We present an optimized linear algorithm for the spatial nonuniformity correction of a CCD color camera's imaging system and the experimental methodology developed for its implementation. We assess the influence of the algorithm's variables on the quality of the correction, that is, the dark image, the base correction image, and the reference level, and the range of application of the correction using a uniform radiance field provided by an integrator cube. The best spatial nonuniformity correction is achieved by having a nonzero dark image, by using an image with a mean digital level placed in the linear response range of the camera as the base correction image and taking the mean digital level of the image as the reference digital level. The response of the CCD color camera's imaging system to the uniform radiance field shows a high level of spatial uniformity after the optimized algorithm has been applied, which also allows us to achieve a high-quality spatial nonuniformity correction of captured images under different exposure conditions.

OCIS codes: 040.1490, 040.1520, 100.2000, 110.4190, 110.4280.

1. Introduction

CCD cameras are the most outstanding sensor devices in generic scientific imaging owing to their high resolution, high quantum efficiency, broad spectral response, acceptable signal-to-noise ratio, linearity, geometric fidelity, rapid response, small size, and durability.[1,2] In spite of this, CCD cameras are not perfect detectors when they are used as instruments for accurate radiometric measurements. Several noise sources such as dark current, shot noise, read noise, quantization noise, and fixed pattern noise, which are inherent in the camera's performance,[2] alter the digital levels corresponding to each pixel, distort the real image acquired in an unknown manner, and degrade radiometric precision, image quality, and resolution. These noise sources and their nature have been widely studied and analyzed.[1–5]

The authors are with the Centre for Sensors, Instruments and Systems Development (CD6), Department of Optics and Optometry, Technical University of Catalonia, Rambla Sant Nebridi 10, 08222 Terrassa, Spain. M. de Lasarte's e-mail address is marta.lasarte@oo.upc.edu.

Received 3 November 2005; revised 3 March 2006; accepted 13 September 2006; posted 13 September 2006 (Doc. ID 65801); published 21 December 2006.

0003-6935/07/020167-08$15.00/0

In fields such as astronomy, it is customary to specify the detected signal and all noise sources in units of equivalent electrons at the detector output because of very low light conditions. The equivalence between the signal electrons generated and the digital levels (DLs) given by the camera's gain constant $K(e\text{-}/\mathrm{DL})$, in addition to the fact that most of the applications of imaging systems based on a CCD camera for standard photometric and colorimetric measurement purposes and most of the nonuniformity correction techniques use digitized images, led us to perform our analysis directly in terms of digital levels, since these constituted the direct response we obtained from the CCD camera. Moreover, the statistics associated with DLs are governed by the photoelectron counting statistics, which constitute a fundamental limit in the photometric performance of a CCD imaging system.

It is essential to correct the spatial nonuniformity of the response of an imaging system based on a CCD color camera if it is to be used as a high spatial resolution instrument for measuring and if the camera's entire detection area is to be made available. Two types of techniques are generally used to perform spatial nonuniformity correction.[6]

The techniques of the first type are based on detector calibration using two images (a dark image and a uniform field image), which are combined linearly with the image to be corrected. These techniques aim to perform accurate radiometric measurements using a

CCD sensor; they are variously referred to as flat fielding, shading correction, flat-field correction, or nonuniformity correction. Hereinafter we refer to them as flat-field correction.

Other techniques are based on the application of an algorithm to an original image in order to provide a considerable improvement in the image quality at the expense of radiometric accuracy. These techniques are usually referred to as scene-based techniques and there are a wide variety of them, such as those that use statistical algorithms,[7] motion-based algorithms,[8] algebraic algorithms,[9] and the inverse covariance form method.[10] A correction technique that combines calibration and an algebraic algorithm, which enables a scene-based radiometrically accurate correction to be achieved, has also been developed.[11,12] Recently, modern vector filtering techniques for color images have been applied to noise removal.[13] One field of application of these techniques is astronomy, as calibration images are not available and high-quality images are required.[14–16]

The goal of our research is to optimize a linear algorithm that allows a CCD camera-based imaging system to be used as a measuring instrument that has high spatial resolution. Therefore high radiometric accuracy is required. Consequently, this study is focused on techniques of the first type mentioned above, as our main objective is to achieve the best flat-field correction of the imaging system.

There are basically two ways of applying the flat-field correction technique. Both require two images: a dark image, captured under the same conditions (exposure time and temperature) as the image to be corrected and with the camera shutter closed, and a flat-field image.

In the first,[2,17,18] the flat-field image corresponds to an image of a uniform gray card placed at the exact location where the images will subsequently be captured and therefore captured under the same illumination and exposure conditions. If we assume that the image corresponding to the gray card is completely uniform, we can use it to numerically compensate for the spatial nonuniformity effect[19] on each of the images captured by the system. In this case, the spatial nonuniformity of both the scene illumination and the device's response contribute to the spatial nonuniformity of the image. Unfortunately, every change in illumination conditions requires capturing a new gray card image. In addition, the approach does not allow the correction of the spatial nonuniformity of the device response independently.

The second way of applying the flat-field correction consists in using a linear algorithm.[20] In this case, the flat-field image corresponds to the image of a uniform radiance field, which is referred to as the base correction image. The brilliant image, which is defined as the image with the highest DL that does not have any saturated pixels, is generally used as the base correction image.[20,21] The dark image and the base correction image are combined with the image to be corrected by means of two linear algorithms.[22–24] In the first one, the images are combined directly according to the following equation:

$$\mathrm{DL}_c(i,j) = k\,\frac{\mathrm{DL}(i,j) - \mathrm{DL}_0(i,j)}{\mathrm{DL}_B(i,j) - \mathrm{DL}_0(i,j)}, \tag{1}$$

where $\mathrm{DL}_c(i,j)$, $\mathrm{DL}(i,j)$, $\mathrm{DL}_0(i,j)$, and $\mathrm{DL}_B(i,j)$ are the DLs of the (i,j) pixel of the corrected image, original image, dark image, and base correction image, respectively, and k is a calibration constant that can be estimated as the mean DL of the image resulting from the difference between the base correction image and the dark image.

The second linear algorithm is based on calculating the gain and offset matrices[20,21]

$$\mathrm{DL}_c(i,j) = O(i,j) + G(i,j)\mathrm{DL}(i,j),$$

$$G(i,j) = \frac{\mathrm{DL}_B - \mathrm{DL}_0}{\mathrm{DL}_B(i,j) - \mathrm{DL}_0(i,j)},$$

$$O(i,j) = \mathrm{DL}_0 - G(i,j)\mathrm{DL}_0(i,j), \tag{2}$$

where $O(i,j)$ ($i = 1, \ldots, m$ and $j = 1, \ldots, n$) represents the (i,j) element of the correction offset matrix $\mathbf{O}$, $G(i,j)$ represents the (i,j) element of the correction gain matrix $\mathbf{G}$, and DL_0 and DL_B are the reference DL of the dark image and the base correction image, respectively. The mean DL for all of the image's pixels is generally used as the reference DL.[20,21] The size of these matrices (m, n) depends on the number of pixels available on the CCD sensor used (m corresponds to the number of pixels present in a row of the CCD sensor and j to the number of pixels in any column).

The differences between the elements of correction offset matrix $\mathbf{O}$ and gain matrix $\mathbf{G}$ are attributable to slight fluctuations in the responses of the individual pixels. These fluctuations cause the fixed pattern noise that is inherent in the camera's response, which we intend to correct by applying the above-mentioned linear correction algorithm.

Both of the linear algorithms described allow the independent spatial nonuniformity correction of the device's response and do not require the flat-field image to be captured anew if the illumination conditions change. This may be useful in several measurement imaging conditions, such as in the case of images corresponding to self-radiating objects.

As stated previously, in the linear algorithm given by Eqs. (2) the reference digital level and the base correction image that are usually used are the mean digital level and the brilliant image, respectively. Although using these values provided acceptable results, the nonuniformity correction could be significantly improved by applying the linear algorithm using other values. The study of the influence of these algorithm variables on the correction and their optimum values is presented in this paper, together with the experimental methodology

developed as a result. The variables studied are the dark image, which can have a zero or nonzero value, the base correction image, which can be different from the brilliant one used thus far, and the reference DLs, which can be different from the mean commonly used. Once the optimized algorithm for the spatial nonuniformity correction of a CCD camera was obtained, the range of application of this spatial characterization was determined by analyzing its performance for several exposure time ranges.

This paper is organized as follows: The experimental methodology developed and the material needed for its application are detailed in Section 2. The results of applying this experimental methodology and the optimized algorithm are presented in Section 3. The most relevant conclusions are discussed in Section 4.

2. Material and Method

To obtain a uniform radiance field, we manufactured an integrator cube, whose sides were 50 cm long and which had an 18 cm × 18 cm window of a white translucent diffuser material on one of its sides. A light source (Philips 150 W halogen lamp) connected to a power supply (Hewlett Packard 6642A DC) for stable illumination was placed at the center of the cube. The sides of the integrator cube were painted white to increase the light diffusion, and a white baffle that did not let the direct light of the lamp reach the window was also used. This baffle was placed parallel to the window at the center of the cube, and the light source was fixed at the center of the baffle on the side opposite the cube window. Consequently, the window of the cube acted as a uniform radiance field and had a spatial variation percentage of 0.50% over the 10 cm × 8 cm centered region that constituted the camera's viewing field. This spatial variation percentage was determined by measuring the radiance over the camera's viewing field region by using a telespectroradiometer (PhotoResearch PR650 with a MS-75 objective lens, and 1° aperture) (Fig. 1).

Our image capturing system was composed of a QImaging QICAM 10 bit color CCD camera attached to a 16 mm, 1:1.4 Cosmicar Television objective lens.

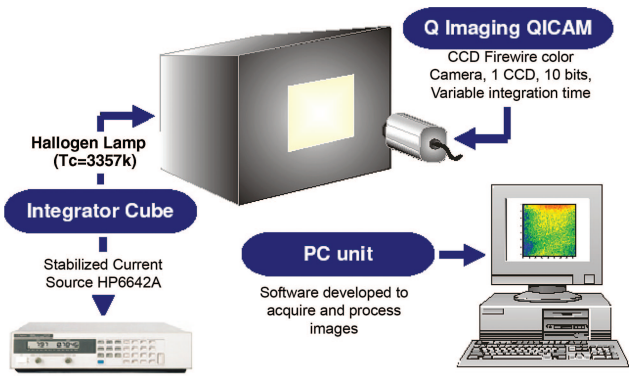

Fig. 1. (Color online) Experimental setup for the spatial characterization of a CCD camera's imaging system.

The CCD sensor used had the spatial resolution of 1024 × 1360 pixels, and a red-green-blue (RGB) Bayer color filter array (CFA).[25] The CFA image captured was demosaicked, and one image was obtained for the R and B acquisition channels, and two images were obtained for the G acquisition channel, which were averaged to obtain one final image. Spatial interpolation was not performed in this case, and, as a result, the spatial resolution of the final images for the R, G, and B acquisition channels was 518 × 680 effective pixels.

The spatial nonuniformity correction of the imaging system was carried out by using images captured from the uniform radiance field and for different exposure levels that were modified by varying the exposure time of the CCD sensor, since the radiance level of the integrator cube was fixed.

The quality of the spatial nonuniformity correction performance was evaluated in terms of the spatial nonuniformity of the digital level of an image of the uniform radiance field, which can be quantified in different ways.[1] In this paper we quantified it by means of Eq. (3), and we hereinafter refer to it as the spatial nonuniformity percentage (SNUP):

$$\mathrm{SNUP} = 100\,\frac{\sigma(\mathrm{Mean})}{\mathrm{Mean}}, \tag{3}$$

where Mean represents the mean digital level of all the image's pixels, and σ(Mean) is the standard deviation associated with it.

For the CCD camera used in this paper, as for most commercial CCD cameras, the exposure time, the electronic gain of the output amplifier, and the zero electronic offset of the analog-to-digital (A/D) converter were user-variable parameters. This allowed us to set the offset and gain parameters to values that optimized the final spatial nonuniformity correction. The gain and offset parameter values were chosen in a way that enabled the response of the RGB channels to be a linear function of the exposure in a certain exposure range. Furthermore, the values were set to have both zero and nonzero dark images in order to determine their influence on the results. Before the spatial nonuniformity correction was applied, the contribution of different zero-mean noise components to the digitized image of the radiance field was reduced as much as possible by analyzing the variation in the quality of the correction as a function of the number of averaged images, which allowed the number of images that needed averaging to be determined. A simplified noise model for a CCD camera was assumed,[1] which considered the total noise associated with the system as the sum of the contributions of the shot noise (photon shot noise and dark current), the pattern noise (fixed pattern noise and photoresponse nonuniformity), and the floor noise (reset noise, amplifier noise, and quantization noise). Bearing in mind the statistics associated with these noise sources,[1,2] image averaging reduces the contribution of all the random noise sources to image noise

in a factor inversely proportional to the number of averaged images.

After that, the spatial nonuniformity correction was carried out by means of the linear correction algorithm given by Eqs. (2). The quality of the spatial nonuniformity correction was optimized by taking into account different dark images, base correction images, and reference digital levels.

3. Results

A. Selection of Gain and Offset

The R and G channels of the imaging system analyzed were more sensitive than the B channel, which needed much greater exposure to reach saturation. The R and G channels showed a linear response over a certain exposure range for all the gain and offset values set. The B channel's response showed two linear zones with different slopes before it became saturated at certain gain and offset values. This two-slope behavior of the B channel must be avoided if one wishes to use the imaging system for measuring.

To produce a nonzero dark image, the offset value must be higher than 1100, and to generate a linear zone with a unique slope for the camera's response in the B channel, the gain parameter value must be below 1200 (Fig. 2). The camera settings selected for a zero dark image were a gain value of 1000 and an offset value of 850. To obtain a nonzero dark image, an offset value of 1400 and a gain value of 1000 were selected. These values led to a dark image with a mean digital level of 35, which was approximately 4% of the maximum useful (linear response zone) digital level of the 10 bit camera. As shown later in this paper, these gain and offset parameter values produced the best spatially corrected images.

B. Number of Images

To determine the number of images to be averaged, the variation of the SNUP of the resulting image was analyzed as a function of the number of averaged images (Table 1). Several images were captured with a fixed exposure time of 40 ms for all the channels of the CCD camera's imaging system, which provided a mean digital level of 683 for the R channel, 737 for the G channel, and 257 for the B channel.

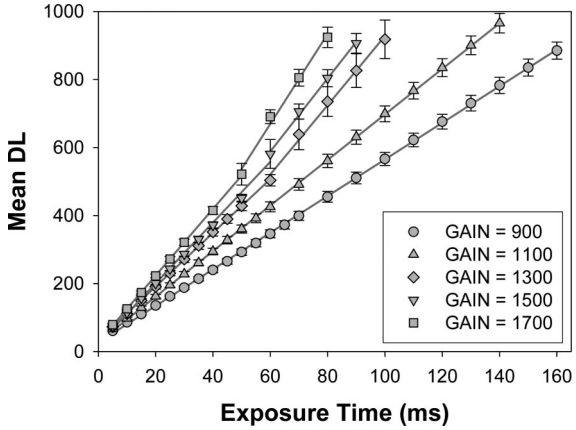

Fig. 2. Mean DL of images from a uniform radiance field for the B channel versus exposure time for different gain values and offset fixed at 1400.

Table 1. SNUP Values and SNUP Reduction Percentages for the Image Resulting from Averaging as a Function of the Number of Averaged Images for the RGB Camera Channels

	R Channel		G Channel		B Channel	
Averaged Images	SNUP	% Reduction	SNUP	% Reduction	SNUP	% Reduction
1	2.6644	–	3.1353	–	3.0815	–
10	2.4957	6.33	3.0850	1.60	2.5654	16.75
20	2.4871	0.34	3.0813	0.12	2.5345	1.20
30	2.4815	0.23	3.0793	0.06	2.5238	0.42
40	2.4805	0.04	3.0790	0.01	2.5156	0.32
50	2.4791	0.06	3.0776	0.05	2.5121	0.14
60	2.4770	0.08	3.0758	0.06	2.5069	0.21

Although progressively increasing the number of averaged images improved the spatial uniformity, using more than 20 images did not lead to a substantial improvement as would be expected since the standard deviation associated with the resulting image, which constituted an approximation to the total noise of the image,[1,2] varied in a manner that was approximately inversely proportional to the square root of the number of averaged images. However, this was not exact since image averaging reduced all random noise sources except those that generated spatial nonuniformity (pattern noise), which, if they were not corrected, would still contribute to image noise. Hereinafter when we refer to an image this means the image resulting from averaging 20 individual, successively captured images.

C. Influence of Dark Image, Base Correction Image, and Reference Digital Level

The linear spatial nonuniformity correction algorithm given by Eqs. (2) was applied to images captured with two different camera gain and offset values, which allowed us to have zero (gain value of 1000 and offset value of 850) and nonzero (gain value of 1000 and offset value of 1400) dark images. We used the image with a mean DL placed in the middle of the useful linear response range of the camera as the base correction image and the mean digital level of the image as the reference digital level.

To analyze the influence of having a zero or nonzero dark image, the spatial nonuniformity correction quality of several corrected images was compared by means of the SNUP (Table 2). The use of a nonzero dark

Table 2. Mean SNUP Values of Images in the Camera's Useful Linear Response Range for Zero Dark Image (ZDI) and Nonzero Dark Image (NZDI) Gain and Offset Settings and for the RGB Camera Channels

	R Channel	G Channel	B Channel
ZDI	0.5162	0.5096	1.8431
NZDI	0.4064	0.3589	0.6280

image improved the spatial nonuniformity correction from 21% up to 66%, depending on the color channel, with respect to corrected images obtained with a zero dark image. Consequently, to obtain images with high spatial nonuniformity correction, it is essential to work with gain and offset values that produce nonzero dark images. Regarding the influence of the base correction image on the quality of the spatial nonuniformity correction, several images were selected: the brilliant image, which is the one usually found in the literature and has the highest mean DL without having any saturated pixels; the central image, which is the image with a mean DL placed in the middle of the useful linear response range of the CCD camera's imaging system; and the extreme image, which is placed at the end of the useful linear response range of the camera and is closest to the brilliant image, although in the camera's linear response range. In this case, as in the analysis of the influence of the dark image, the mean DL of the image was taken as the reference DL. As can be seen in Table 3, using the central and extreme images as base correction images led to a clear improvement in the quality of the spatial nonuniformity correction. The best correction was commonly achieved by using the central image, for which an improvement of the spatial nonuniformity correction of 41% was obtained for the R channel, and an improvement of 29% for the G channel. For the B channel, the results obtained by using the different images selected as base correction images were quite similar. This is probably attributable to the fact that the B channel's response showed two linear zones. Although we modified the gain and offset values to obtain a unique slope, this linear behavior was observed when the average of the entire image was considered. However, the linearity of the individual response of each pixel was not guaranteed, and this may have affected the results.

Although one might think that taking the brilliant image as the base correction image would enable the full response range of the camera to become involved, this image was placed at the beginning of the saturation zone of the camera response, and this might be why the brilliant image led to worse results than the central and extreme images, which were both in the linear response range. Thereafter the base correction image was taken to be the central image.

As in the case of the base correction image, several values were taken as the reference digital level in order to determine its influence on the quality of the spatial nonuniformity correction: the mean DL, which is the one that is usually used; the mode of all the DLs of the pixels in the image; and the digital level corresponding to the central pixel of the image. The central images for each RGB channel were taken as the base correction images.

The results obtained in terms of the spatial nonuniformity correction quality were very similar for all the reference digital levels considered (Table 4). The results corresponding to the mean and mode digital levels were practically identical and slightly better than those obtained for the central digital level. This could be attributable to the statistical nature of these two reference DLs since they are related to the DL value distribution of an image. From this point on, the mean DL is taken as the reference DL in the linear spatial nonuniformity correction algorithm, since it is usually used as the reference DL in the literature.

D. Range of Application of the Spatial Characterization

Up to this point, the illumination conditions were fixed, and, as a result, the exposure time range in which the camera's linear response was useful was also fixed, depending on the gain and offset settings. However, the exposure time range can change depending on the image captured.

The algorithm optimized for spatial characterization [Eqs. (2)] depends fundamentally on the correction gain matrix since the correction offset matrix is

Table 3. Exposure Time Corresponding to Each Base Correction Image and Mean SNUP Values for the RGB Camera Channels[a]

	R Channel		G Channel		B Channel	
	t_{exp} (ms)	Mean SNUP	t_{exp} (ms)	Mean SNUP	t_{exp} (ms)	Mean SNUP
BI	60	0.6914	55	0.5081	155	0.5816
CI	30	0.4064	30	0.3589	80	0.6280
EI	55	0.4307	50	0.3669	150	0.6133

[a]These values are for the spatially corrected images in the camera's useful linear response range, using the brilliant image (BI), the central image (CI), and the extreme image (EI) as the base correction images in the linear spatial nonuniformity correction algorithm.

Table 4. Mean SNUP Values for the RGB Camera Channels of the Spatially Corrected Images[a]

	R Channel	G Channel	B Channel
Mean DL	0.4064	0.3589	0.6280
Mode DL	0.4064	0.3596	0.6289
Central DL	0.4071	0.3606	0.6323

[a]These values are obtained by using the mean DL of the image, the mode of all the pixel's digital levels (mode DL), and the digital level of the central pixel (central DL) as the reference DL in the linear spatial nonuniformity correction algorithm.

Table 5. Radiance and Exposure Time Ranges[a]

RL	Radiance (W/sr m^2)	Exposure Time Range (ms)		
		R Channel	G Channel	B Channel
1	5.2630	5–60	5–50	10–160
2	3.8460	10–80	10–80	10–225
3	2.6620	10–100	10–100	50–400
4	1.7580	25–175	25–175	50–700
5	1.0920	25–300	25–300	100–1300
6	0.6303	50–500	100–700	200–2500

[a]These ranges are the useful linear response ranges for each RGB channel, corresponding to the six radiance levels (RL) considered.

calculated from the correction gain matrix and the dark image captured under the same conditions as the image to be corrected. For this reason, assessing the application of the optimized algorithm to spatial characterization involves determining whether a correction gain matrix calculated for certain fixed illumination conditions, and thus a fixed exposure time range, leads to high-quality spatial nonuniformity correction when it is used to correct an image captured in any other exposure time range, beyond the useful linear response range of the camera.

To check the application of the optimized algorithm to spatial characterization, several groups of images of a uniform radiance field were captured for several radiance levels by varying the current intensity applied to the halogen lamp. A correction gain matrix [$\mathbf{G}^{(i)}$ (i = 1, 2, 3, 4, 5, 6 radiance levels)] was calculated for each radiance level (exposure time range). Each one of these correction gain matrices was used to correct the groups of images corresponding either to its own radiance level or to the rest of the radiance levels considered. The radiance levels were selected on the basis of the exposure time ranges associated with them (Table 5). The selected values corresponded to the useful linear response ranges of the CCD camera's imaging system for each channel. From this point on, when we refer to the radiance level we mean the corresponding exposure time range of the RGB channel responses, rather than the numerical radiance level itself.

The mean SNUP obtained for each radiance level (ranges 1 to 6) as a function of the radiance level of each correction gain matrix used is shown for the different radiance levels in Figure 3, for the RGB chan-

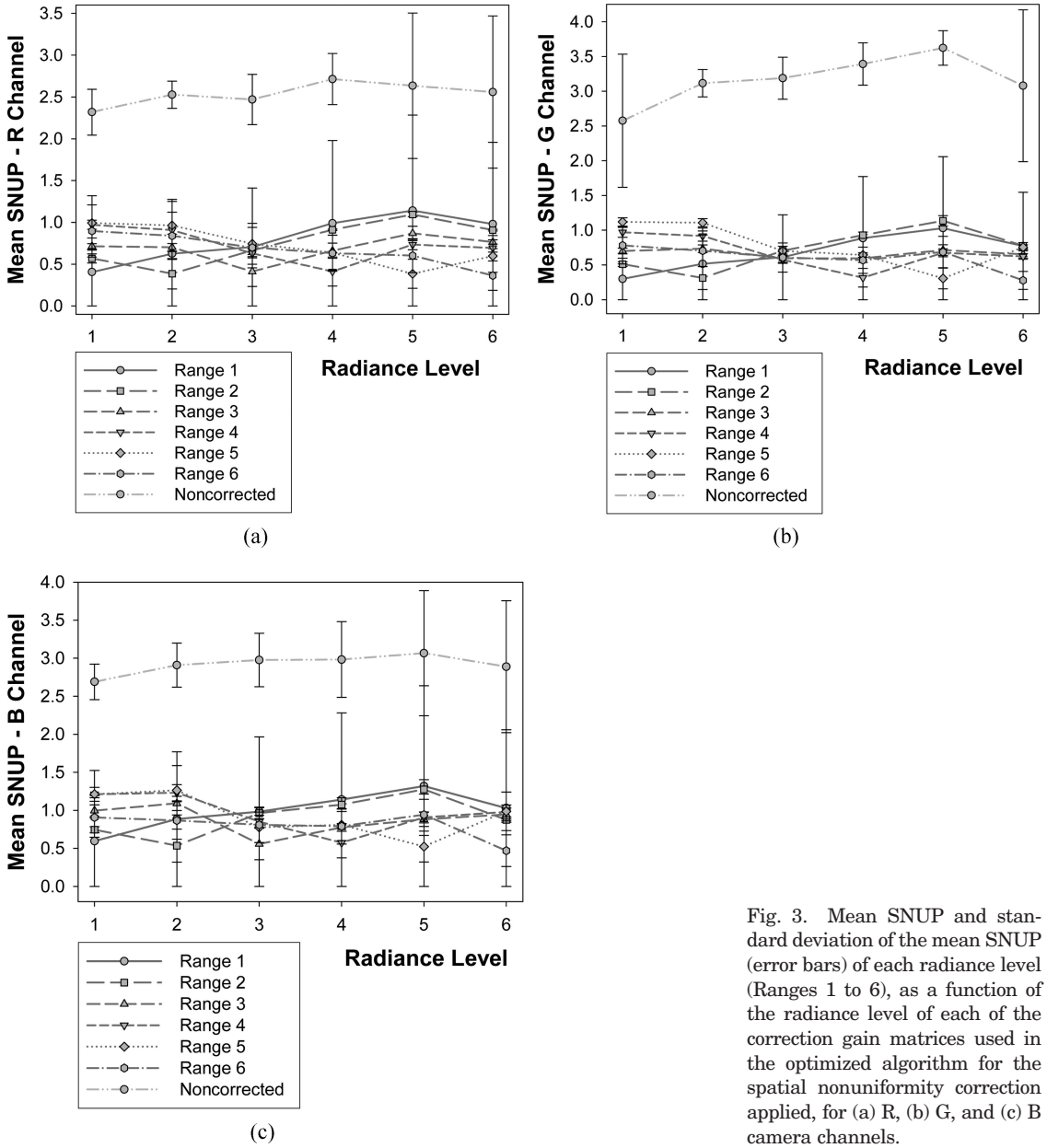

Fig. 3. Mean SNUP and standard deviation of the mean SNUP (error bars) of each radiance level (Ranges 1 to 6), as a function of the radiance level of each of the correction gain matrices used in the optimized algorithm for the spatial nonuniformity correction applied, for (a) R, (b) G, and (c) B camera channels.

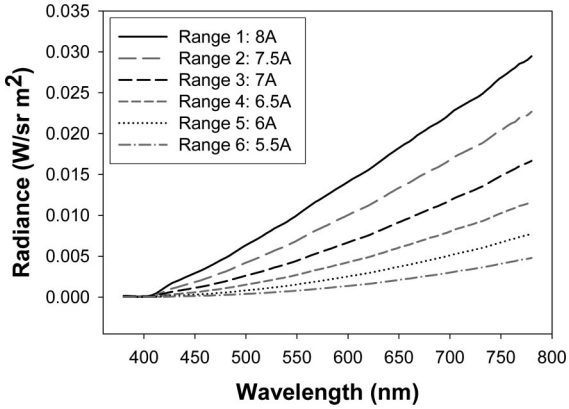

Fig. 4. Radiance spectrum of the incident light in the CCD camera imaging system. Different radiance levels are achieved by varying the intensity of the current applied to the light source.

nels. The mean SNUP of the original, noncorrected images for the different radiance levels is also shown.

The best results were obtained when images corresponding to a radiance level were corrected using the correction gain matrix calculated for the same radiance level or for the radiance levels closest to it. High radiance levels corresponding to low exposure time ranges led to better results than low ones, probably because of the growing effect of dark noise on the camera's response as a result of longer exposure times. In spite of this, if one compares the mean SNUP of the corrected images of different radiance levels by using the gain correction matrices calculated for all the radiance levels with the mean SNUP of the noncorrected images for the same radiance levels, one can see that the calculation of a correction gain matrix at a certain radiance level (preferably a high radiance level) and thus a certain exposure time range of the RGB channels (preferably a low exposure time range) would be sufficient to achieve a high-quality spatial nonuniformity correction of images when the optimized linear spatial nonuniformity correction algorithm is applied to them by using this gain matrix.

Obtaining different radiance levels by varying the current intensity applied to the halogen lamp considerably modified the radiance spectrum of the incident light in the CCD camera's imaging system (Fig. 4). Therefore the fact that high-quality spatial nonuniformity correction of images is achieved for different exposure time ranges proves that the correction performed by this optimized algorithm is independent of changes in the radiance spectrum of the incident light and that the algorithm may be successfully applied under a wide range of exposure conditions.

4. Conclusions

In this paper we have presented an optimized linear algorithm for the spatial nonuniformity correction of a CCD camera's imaging system and the experimental method designed for its implementation.

To use a CCD image capture device as a measuring instrument, its response must be a linear function of exposure within a certain range, for each of the RGB channels. Therefore, all our imaging system's settings (exposure time range, gain, offset, etc.) were chosen to guarantee this linear response.

Before the nonuniformity correction was applied, the contribution of the different zero-mean noise components was minimized by averaging a certain number of images. It was found that an average of 20 images was sufficient to attenuate the effect of these components on the image.

Although the linear correction algorithm considered in this work is common in the literature, it is always applied by using the mean digital level and the brilliant image as the reference digital level and the base correction image, respectively. By using other values, the results published in the literature can be considerably improved, and therefore the algorithm can be optimized. In our research, we studied the influence of the dark image, the base correction image, and the reference digital level in order to optimize the spatial nonuniformity correction.

To obtain the best spatial nonuniformity correction quality, a nonzero dark image is needed, which, in the case of the imaging system used, improved the spatial nonuniformity correction from 21% up to 66% depending on the color channel, with respect to the corrected images obtained when a zero dark image was used.

We showed that the best correction was achieved by using the central image, i.e., the image with a mean digital level placed in the middle of the useful linear response range of the camera, as the base correction image. In the case of the imaging system used, an improvement of the spatial nonuniformity correction of 41% for the R channel and of 29% for the G channel was achieved by using the central image instead of the brilliant image.

With regard to the reference digital level, the mean and the mode of all the pixel digital levels of an image gave practically identical results. Because the mean digital level of the image is the one that is most commonly used, we selected it as the reference digital level.

Finally, the application of the spatial characterization developed was assessed by capturing groups of images for different radiance levels, calculating the correction gain matrix for each radiance level and correcting the images of all the radiance level groups with the correction gain matrices calculated for each radiance level. The best results were obtained when images corresponding to a radiance level were corrected by using the gain matrix calculated for the same radiance level or for those closest to it. In spite of this, the comparison between the mean SNUP of corrected and noncorrected images showed that calculating a unique correction gain matrix at a certain radiance level would be sufficient to achieve a high-quality spatial nonuniformity correction of images of different radiance levels. High radiance levels corresponding to low exposure time ranges were preferred for calculating the gain correction matrix since these led to better results than did low levels.

References

1. G. C. Holst, *CCD Arrays, Cameras, and Displays* (SPIE Press, 1996).
2. J. R. Janesick, *Scientific Charged-Coupled Devices* (SPIE Press, 2001).
3. G. E. Healey and R. Kondepudy, "Radiometric CCD camera calibration and noise estimation," IEEE Trans. Pattern Anal. Machine Intell. **16,** 267–276 (1994).
4. "CCD Image Sensor Noise Sources," Application Note, Image Sensor Solutions, Eastman Kodak Company (2001), http://www.kodak.com/go/imagers.
5. P. E. Haralabidis and C. Pilinis, "Linear color camera model for a skylight colorimeter with emphasis on the imaging pipeline noise performance," J. Electron. Imaging **14,** 043005 (2005).
6. B. M. Ratliff, M. M. Hayat, and J. Scott Tyoc, "Algorithm for radiometrically-accurate nonuniformity correction with arbitrary scene motion," J. Opt. Soc. Am. A **20,** 1890–1899 (2003).
7. M. M. Hayat, S. N. Torres, E. E. Armstrong, and B. Yasuda, "Statistical algorithm for nonuniformity correction in focal-plane arrays," Appl. Opt. **38,** 772–780 (1999).
8. R. C. Hardie, M. M. Hayat, E. E. Armstrong, and B. Yasuda, "Scene-based nonuniformity correction using video sequences and registration," Appl. Opt. **39,** 1241–1250 (2000).
9. B. M. Ratliff, M. M. Hayat, and R. C. Hardie, "An algebraic algorithm for nonuniformity correction in focal-plane arrays," J. Opt. Soc. Am. A **19,** 1737–1747 (2002).
10. S. N. Torres, J. E. Pezoa, and M. M. Hayat, "Scene-based nonuniformity correction for focal plane arrays by the method of the inverse covariance form," Appl. Opt. **42,** 5872–5881 (2003).
11. B. M. Ratliff, M. M. Hayat, and J. S. Tyo, "Radiometrically-calibrated scene-based nonuniformity correction for infrared array sensors," in *Infrared Technology and Applications XXVIII,* B. F. Anderson, G. F. Fulop, and M. Strojnik, eds., Proc. SPIE **4820,** 359–367 (2003).
12. B. M. Ratliff, M. M. Hayat, and J. Scott Tyo, "Radiometrically accurate scene-based nonuniformity correction for array sensors," J. Opt. Soc. Am. A **20,** 1890–1899 (2003).
13. R. Lukac, B. Smolka, K. Martin, K. N. Plataniotis, and A. N. Venetsanopoulos, "Vector filtering for color imaging," IEEE Signal Process. Mag. **22,** 74–86 (2005).
14. I. T. Young, J. J. Gerbrands, and L. J. v. Vliet, "Image processing fundamentals," in *The Digital Signal Processing Handbook,* V. K. Madisetti and D. B. Williams, eds. (CRC Press in cooperation with IEEE Press, 1998), pp. 51.1–51.81.
15. A. V. Oppenheim, R. W. Schafer, and T. G. Stockham, Jr., "Non-linear filtering of multiplied and convolved signals," Proc. IEEE **56,** 1264–1291 (1968).
16. H. J. A. M. Heijmans, *Morphological Image Operators* (Academic, 1994).
17. R. S. Berns, "The science of digitizing paintings for color-accurate image archives: a review," J. Imaging Sci. Technol. **45,** 305–325 (2001).
18. J. A. Tyson, "Low-light-level charge-coupled device imaging in astronomy," J. Opt. Soc. Am. A **12,** 2131–2138 (1986).
19. M. Thomson and S. Westland, "Colour-imager characterization by parametric fitting of sensor responses," Color Res. Appl. **26,** 442–449 (2001).
20. R. Aikens, D. A. Agard, and J. W. Sedat, "Solid-state imagers for microscopy," Methods Cell Biol. **29,** 291–313 (1989).
21. L. Bellia, A. Cesarano, F. Minichiello, S. Sibilio, and G. Spada, "Calibration procedures of a CCD camera for photometric measurements," presented at IMTC 2003—Instrumentation and Measurement Technology Conference, Vail, Colo., 20–22 May 2003.
22. L. J. van Vliet, F. R. Boddeke, D. Sudar, and I. T. Young, "Image detectors for digital image microscopy," in *Digital Image Analysis of Microbes; Imaging, Morphometry, Fluorometry and Motility Techniques and Applications, Modern Microbiological Methods,* M. H. F. Wilkinson and F. Schut, eds. (Wiley, 1998), pp. 37–64.
23. "Image Calibration," Roper Scientific, 2004, retrieved September 2005, http://www.roperscientific.de/timagecal.html.
24. J. M. Arneson, "CCD optimization the limits of deep-sky imaging," Macalester College, retrieved September 2005, http://www.macalester.edu/astronomy/research/phys40/jon/webpage.html.
25. R. Lukac and K. N. Plataniotis, "Color filter arrays: design and performance analysis," IEEE Trans. Consum. Electron. **51,** 1260–1267 (2005).